Effects of Functionalized MWNTs with GMA on the Properties of PMMA Nanocomposites

Yaping Zheng, Jiaoxia Zhang, Yang Xiaodong, Weiwei Chen, Rumin Wang

Department of Applied Chemistry, School of Natural and Applied Science, Northwestern Polytechnical University, Xi'an, 710072, People's Republic of China

Received 6 May 2008; accepted 4 September 2008
DOI 10.1002/app.29303
Published online 11 February 2009 in Wiley InterScience (www.interscience.wiley.com).

ABSTRACT: The acid modification of multiwall carbon nanotubes (MWNTs) was performed by an HNO_3/H_2SO_4 solution. The glycidyl methacrylate (GMA) undergoing an opening-ring was grafted onto the surface of acid-modified MWNTs. The surface properties of MWNTs were investigated by Fourier transform infrared spectrometer (FTIR), Raman spectra, transmission electron microscopy (TEM), X-ray diffraction, and thermogravimeric analysis. Then the MWNTs/ poly(methyl methacrylate) (PMMA) nanocomposites were prepared by *in situ* polymerization. The tribological and dielectric properties of nanocomposites were studied. As a result, GMA was grafted on the surface of MWNTs. The tribological and dielectric properties of MWNTs/ PMMA nanocomposites were improved as the content of the surface-modified MWNT increased. The marked improvement in tribological and dielectric properties were attributed to the good dispersion of MWNTs that were bonded with C=C on the surface that participated in the polymerization of MMA. © 2009 Wiley Periodicals, Inc. J Appl Polym Sci 112: 1755–1761, 2009

Key words: carbon nanotubes; glycidyl methacrylate; surface modification; nanocomposites

INTRODUCTION

Carbon nanotubes (CNTs) exhibiting exceptionally mechanical properties,[1–3] a high aspect ratio and huge specific surface areas (SSA) of up to $>1300\ m^2/g$,[4] in combination with an electrical and thermal conductivity make them a good reinforcing material with conductive performance in polymer matrix and open up new perspectives for multifunctional materials.[5]

But mechanical reinforcement of CNTs as a structural element in polymers is difficult and faces a challenging task. To efficiently exploit the potential properties of CNTs and improve the performance of polymer matrix, the effect behaviors must be taken to solve (i) aggravated challenges of CNTs due to the high SSA and quite strong van der Waals forces among themselves and (ii) the weaker interfacial adhesion between the CNTs and the polymer matrix.[6–8]

Therefore, to enhance their compatibility, extensive research is focused on surface modification of CNTs.[9–12] The chemical modification of the open ends, the exterior walls (convex face), and the interior cavity (concave face) of the CNTs is expected to play a vital role in tailoring the properties of these materials and the engineering of nanotubes devices.[13] The chemical modification includes noncovalent and covalent modification, which can improve their chemical compatibility. The noncovalent modification of CNTs embody noncovalent coating with surfactants,[14,15] wrapping and adsorbing the long-chain polymers such as polystyrene sulfonate,[16] poly(vinyl alcohol),[17] and poly(ethylene oxide).[18] However, the dispersion of CNTs subjected to noncovalent bond modification is unstable and unable to undergo further modification, resulting in limited applications.

In the covalent modification, the long alkyl chains, polymer chains, and biomolecules can be grafted onto the graphite surface, end cups and structural defects of CNTs. The covalent modification can be performed through esterification and amidation reactions[19–21] such as polyetherimides,[22] poly(aminobenzene sulfonic acid),[23] and hyperbranched polymers.[24] The covalent modification of CNTs often alters slightly the structure and damages corresponding properties of CNTs, but it is able to improve greatly the solubility and compatibility of CNTs.

Poly(methyl methacrylate) (PMMA) is a very important thermoplastic because of its favorable mechanical and dielectric properties, good solvent resistance, and outstanding climate resistance. Now PMMA is widely used in architecture, automotive, air and railway transport systems for tribological applications.[25]

Correspondence to: Y. Zheng (zhengyp@nwpu.edu.cn).
Contract grant sponsor: Shaanxi Natural Science Funds 2007; contract grant number: 2007E108.
Contract grant sponsor: Doctorate Foundation of Northwestern Polytechnical University; contract grant number: CX200816.
Contract grant sponsor: NPU Science Research Startup Fund.

However, the difficulty in the worse tribological performance applications limits some applications of PMMA.[26] Because of the effects of the reinforcement of CNTs, PMMA nanocomposites with excellent tribological properties can be fabricated with CNTs.

Recently, Yang et al.[27] prepared CNTs/PMMA nanocomposites through *in situ* polymerization. Du et al.[28] obtained a better dispersion of single wall carbon nanotubes in PMMA polymer matrix by a coagulation method. Zhu et al. investigated the impact strength of CNTs/PMMA nanocomposites prepared by *in situ* polymerization. CNTs were first treated by strong acid to exhibit surface organic activity. They observed the impact strength of the nanocomposites increased by >80%, when the content of CNTs was 1.0%.[29] Because the surface characteristics of the CNTs differ markedly from those of the PMMA, the nanocomposites may exhibit phase separation as time passes. In this study, strong acid treatments were performed on multiwall carbon nanotubes (MWNTs), then GMA was grafted onto the sidewall of acidified MWNTs through interactions between epoxy group of GMA and carboxylic acid groups. MWNTs/PMMA nanocomposites were prepared through a conventional *in situ* bulk polymerization. At last, the effects of functionalized MWNTs on tribological and dielectric properties of these nanocomposites were analyzed and discussed.

EXPERIMENT

Materials

The MWNTs used in this study were synthesized by chemical vapor deposition and provided by Chengdu organic chemicals Co., Ltd. The diameter was 20–30 nm with micrometers length, and the purity was >95 wt %. The MWNTs were used in our experiment without further purification.

Nitric acid (70%) and sulfuric acid (98%) were obtained from Xi'an Jingpu Fine Chemical Company. Glycidyl methacrylate (GMA, purity >90%) was purchased from Beijing Yanshan synthesizing material company. The analytical grade Catalyst (CT-3) was obtained from Tianjing Synthesis Materials Company. Methyl methacrylate (MMA, analytical reagent) was produced by Tianjing Botong Chemical Company and was dried and purified by distilling under reduced pressure. The free radical initiator, azodiisobutyronitrile (AIBN, analytical reagent) was obtained from Hongsheng Chemical Company.

Surface treatment method and preparation of nanocomposites

The MWNTs (1 g) were sonicated in a mixture of concentrated H_2SO_4 and HNO_3 (3 : 1 by volume) at 60°C and 55 kHz for 30 min. The black suspended substances were immersed in an oil bath and refluxed for 12 h. Then the black solution containing MWNTs was filtered through 2 μm millipore polycarbonate membrane, and washed constantly by distilled water to remove any acid until the pH = 7 of the MWNTs in water. Dried at 80°C under vacuum for 24 h, $MWNT_{COOH}$ were obtained.

Surface treatment of $MWNT_{COOH}$ with GMA was carried out as follows: GMA (35 g) and $MWNT_{COOH}$ (500 g) were mixed in the 100 mL beaker with the high-speed dispersion homogeneous machine for 30 min. The suspended substances were poured into boiling flask-three-neck. The flask was immersed in an oil bath at 120°C. Catalyst (35 mg) was added into the flask, and then the mixture was stirred for 1.5 h at 120 ± 5°C, diluted with $CHCl_3$ at last, and vacuum filtered using a 0.22 μm polycarbonate membrane. The filtered mass was dispersed in $CHCl_3$, then filtered and washed with $CHCl_3$. After drying overnight under vacuum at 80°C, $MWNT_{GMA}$ were finally obtained.

Typically, the $MWNT_{GMA}$/PMMA nanocomposites were prepared by *in situ* polymerization. First, the appropriate amount of $MWNT_{GMA}$ and 30 g of purified MMA monomer were mixed by a high-speed homogenizer for 30 min leading to a homogeneous dispersion of $MWNT_{GMA}$ in MMA. The rotation speed was fixed at 15,000 rpm in our experiment. After dispersion, the mixture was placed into the boiling flask-three-neck and removed the air by N_2. Then the free radical initiator, AIBN (0.1 wt %) was added into the flask to initiate the free radical under stirring. With the initiation of the free radicals, the C=C double bonds in MMA molecules were opened, and then linked each other to form long chain of PMMA molecules.[8] The reaction lasted for 30 min at 75 ± 5°C. Then the mixture was cooled once and quickly poured into a preheated steel mold coated. The mold enclosed resulting mixture was degassed at room temperature under vacuum for 30 min to remove bubbles. After removing bubbles, the mixture was heated to 50°C, held for 30 h, then stepped up to 100°C for 2 h, and finally cooled to room temperature in the mold. The samples were incised according to standard. The contents of $MWNT_{GMA}$ were 0, 0.5, 1, 2, and 5 wt % (weight percent with respect to MMA monomer).

Measurements and characterizations

The groups of the MWNTs and functionized MWNTs were investigated by Fourier transform infrared spectrometer (FTIR, WQF-310, Beijing second opitics instrument, China).

X-ray diffraction (XRD) analysis was recorded by monitoring the diffraction angle (2θ) from 10° to 80°on a Scintag D/MAX-3C diffractometer (Rigaku

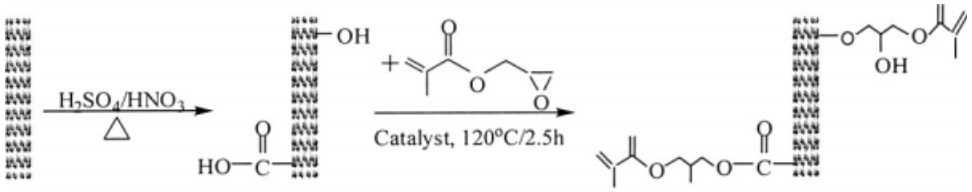

Figure 1 Reaction scheme of surface function treatment for MWNTs.

Co., Japan) equipped with a Ni-filtered Cu Ka radiation ($\lambda = 1.54$ Å) source operated at 40 kV and 20 mA.

Thermogravimeric analysis (TGA) measurements were taken under N_2 flow using TGAQ50 instrument (TA Co.) at a heating rate of 10°C /min and a nitrogen flow of 50 cm^3/min.

Transmission electron microscope (TEM) examinations were conducted on the Joel H-600 instrument (Hitachi Co., Japan) at an accelerating voltage of 100 kV. The sample was prepared through depositing a drop of the dispersion solution of MWNTs in water on a TEM grid (300 mesh Cu grid).

Scanning electron microscope (SEM) examinations were observed on the AMRAY-1000B instrument (AMRAY Co.) SEM at 5.0 kV. The specimens were coated with gold vapor to make them conducting.

Raman spectroscopy was carried out at room temperature using an ALMEGA Raman spectroscope (Nicolet) equipped with a 532 nm TUIOptics laser and a displacement range of 800–4000 cm^{-1}.

The dielectric constant (ε) and dielectric loss tangent (tan δ) of the nanocomposites were measured using an AS2586 (Shanghai Angle Electronic Co., China) equipped with high frequency Q cooperate instrument S914 at room temperature. Testing frequency was 1 MHz, and sample size was 27 × 27 × 4 mm^3.

Abrasion properties of nanocomposites were tested at MM-200 Abrasion Instrument (Jinan Testing Machine Factory, China). The sample size was 30 × 7 × 6 mm^3. A steel ring was rotated against the nanocomposites at speeds of 200 r/min and load of 320–620 N. The sliding time of 120 min was used in all friction tests. Before each test, the steel ring was abraded with 900 grade water proof abrasive paper. Then the steel ring was cleaned with acetone followed by drying.

RESULTS AND DISCUSSION

The properties of MWNTs could be significantly improved by oxidation of strong acids mixture including H_2SO_4 and HNO_3. After acid treatment, there are carboxylic groups on the end caps of the MWNTs. The GMA-functionalized MWNTs were obtained according to Figure 1, where surface-bound —COOH and —OH groups are converted into GMA groups and subsequently reacted with MMA.

Figure 2 shows the FTIR spectrum diagram of MWNTs before and after surface treatment. After treating the MWNTs with mixed strong acids, $MWNT_{COOH}$ exhibits a band at 1634 cm^{-1} assigned to the stretching vibrations of the —COOH groups, and a band at 3400 cm^{-1} attributed to the —OH stretching vibrations. It indicates that there are some —COOH

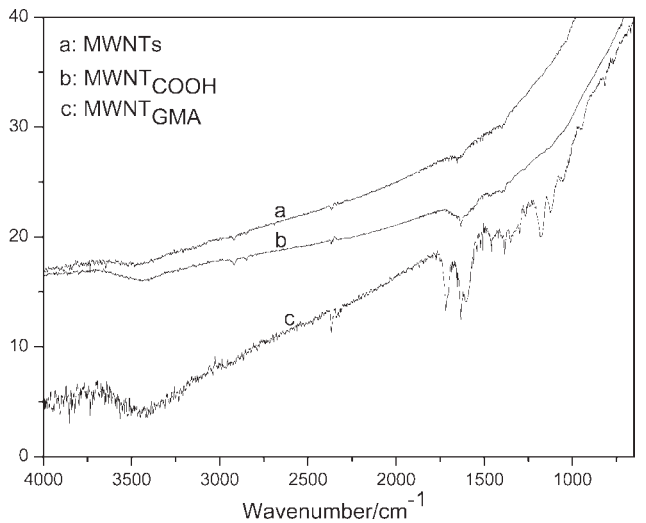

Figure 2 The FTIR spectrum diagram of MWNTs before and after treatment.

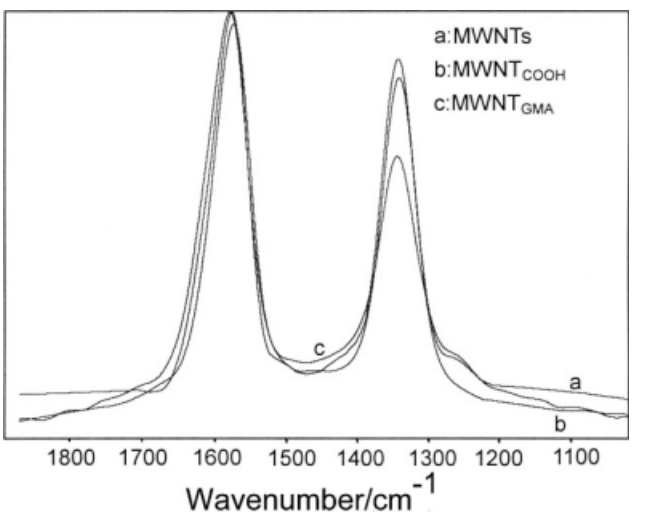

Figure 3 The Raman spectrum diagram of MWNTs before and after treatment.

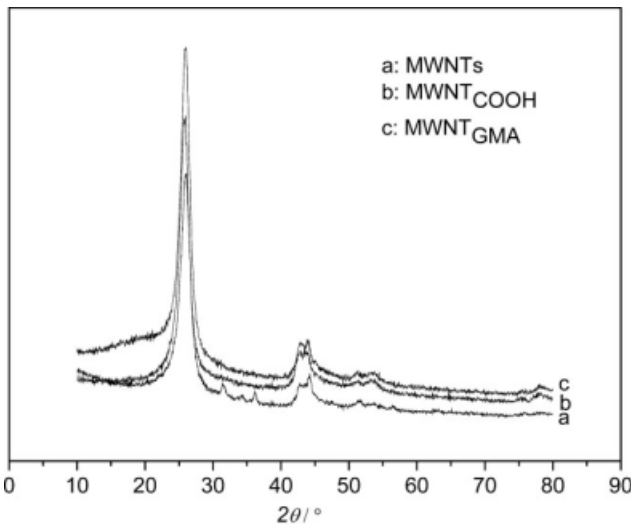

Figure 4 The X-ray diffraction curve of before and after treatment.

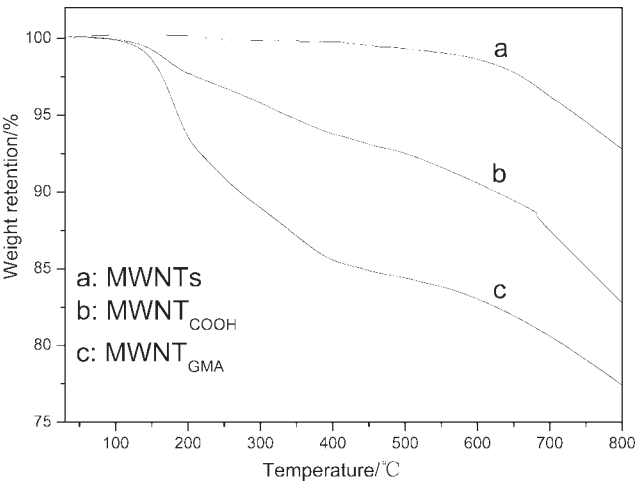

Figure 5 The TGA curves of (a) MWNTs and (b) $MWNT_{COOH}$, and (c) $MWNT_{GMA}$.

and —OH groups on the surface of MWNTs. In the treatment, mixed strong acids releases free oxygen atoms, and mixed strong acids can make carbon atoms become active.[30] The free oxygen atoms and active carbon atoms can form —COOH and —OH groups on the surface of MWNTs. After $MWNT_{COOH}$ was treated with GMA, there is a band 1750 cm^{-1} attributed to the —COOH groups of $MWNT_{GMA}$. In addition, $MWNT_{GMA}$ exhibits a band at 1625 cm^{-1} attributed to double bond. It is known from the carboxyl and double bond that GMA had covalently bonded on the surface of MWNTs through ring-opening reaction.

Figure 3 shows the Raman spectrum diagram of MWNTs before and after surface treatment. In the peaks of the Raman spectra, the main peak at 1578 cm^{-1} is the G pattern of the tangent carbon contradiction vibration of MWNTs. The 1343 cm^{-1} peak is the D pattern induced by the defects of MWNTs. It is known from the diagram that the Raman spectrum of the MWNTs and the $MWNT_{COOH}$ is extremely similar. The softening phenomenon of the phonon pattern near 1578 cm^{-1} is not observed. This is in agreement with theoretical computing results of the lattice kinetics. The theoretical computation predicts that the phonon of MWNTs has no apparent softening when the diameter is in the range of 10–20 nm.[31] The peak of the D pattern of $MWNT_{GMA}$ is lowered distinctly. This may be the cause that after treatment, the organic molecules of $MWNT_{GMA}$ bring about a disorder augmentation.

Figure 4 displays the XRD curves of the MWNTs before and after modification. From curve *a*, it can be seen that there are strong peaks at $2\theta = 25.958°$ ($d = 0.343$ nm), and a weak peaks at $2\theta = 44.280°$

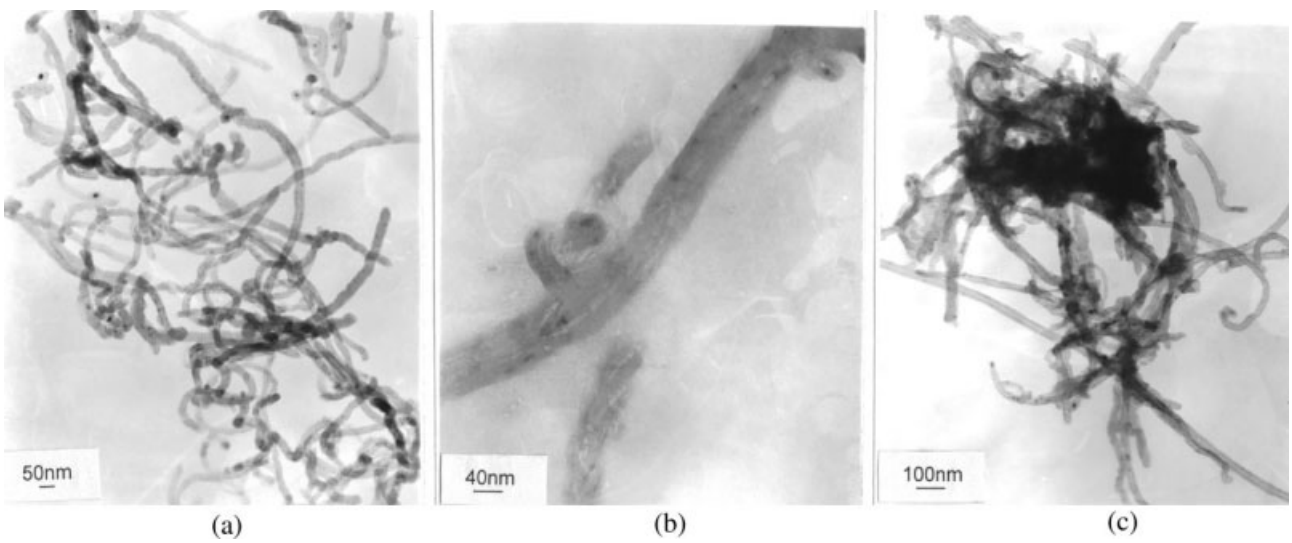

Figure 6 TEM images of (a) MWNTs, (b) $MWNT_{COOH}$, and (c) $MWNT_{GMA}$.

(d = 0.205 nm). This tallies with characteristic peaks of the graphite on the (002) plane and (100) plane. It verifies that MWNTs have the similar structure with graphite. The appearance of hybrid peaks at 2θ = 31.517° and 2θ = 31.167° may result from the influence of the catalyst remaining when preparing MWNTs. When the diffraction angle of the acidified $MWNT_{COOH}$ is 2θ = 25.880° (d = 0.3427 nm) and 2θ = 43.660° (d = 0.2023 nm), the hybrid peaks disappear when compared with the pure MWNTs. The peak at 2θ = 25.880° increases remarkably. This implies that the strong acid treatment may purify and refine the MWNTs. The diffraction angle of $MWNT_{GMA}$ are 2θ = 25.840° (d = 0.3435 nm) 2θ = 43.853° (d = 0.2043 nm). Compared with acidified MWNTs, the peak is reduced and there is little change in the location of the diffraction peak. The change in the peaks may come from the hybridization caused by the polymers wrapped on the wall of MWNTs.

To estimate the effects of surface modification on the thermal stability of the MWNTs, thermal scans of MWNTs. $MWNT_{COOH}$ and $MWNT_{GMA}$ were carried out from 25 to 800°C by the TGA in nitrogen atmosphere (Fig. 5). It can be seen that the weight loss of MWNTs at 650°C is negligible. The $MWNT_{COOH}$ shows weight loss around 185°C, which corresponds to the degradation of the functional groups (—COOH, —OH) on the surface. The weight loss percent is up to 10% at 650°C. The broad degradations of $MWNT_{GMA}$ observed at higher temperatures (>500°C) are related to the thermal decomposition. Weight loss content of 18% from the thermograms indicates the degradation of GMA.

Figure 6 gives the TEM images of MWNTs before and after treatment. It is clear that the tube wall of the MWNTs gets coarse and be cut off. After GMA treatment, the surface of $MWNT_{GMA}$ becomes coarse and there is modification polymer on it. This suggests that GMA is effectively grafted onto the MWNTs surface.

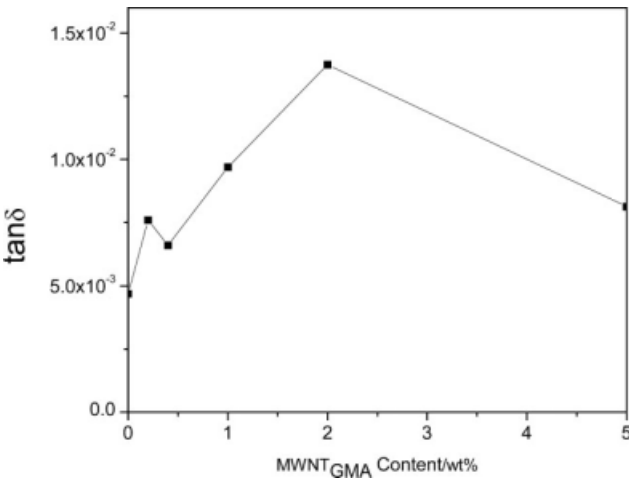

Figure 8 The effect of $MWNT_{GMA}$ contents on dielectric dissipation factor of nanocomposites.

Figures 7 and 8 give respectively the change of the dielectric constant and dielectric loss of the PMMA nanocomposites with the increase of $MWNT_{GMA}$ content. It can be seen from Figure 7 that the dielectric constant of the $MWNT_{GMA}$/PMMA nanocomposites gradually increases with the $MWNT_{GMA}$ content is 0.5%. Then the dielectric constant decreases, when the $MWNT_{GMA}$ content is 1%. When the content of the $MWNT_{GMA}$ is 2%, the dielectric constant is increased from 2.43 of the pure system to 2.99. When the content of $MWNT_{GMA}$ further increases, the dielectric constant decreases once again. The dispersion of $MWNT_{GMA}$ affects the dielectric constant of nanocomposites. $MWNT_{GMA}$ is electrical network structure. When $MWNT_{GMA}$ is dispersed well in polymer, it can form more electrical network structure in the nanocomposites, leading to the heightening of the

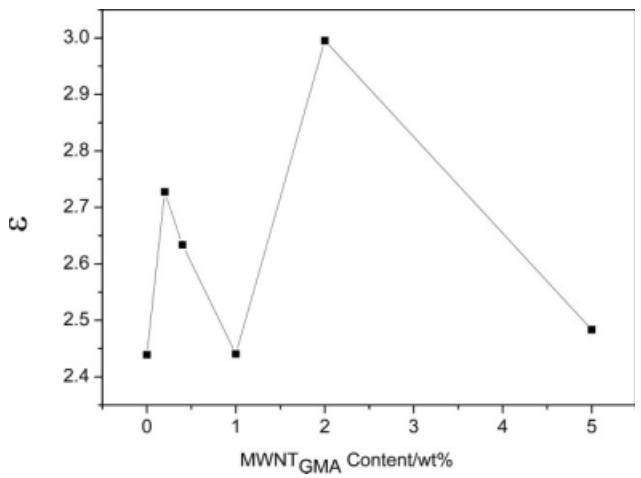

Figure 7 The effect of $MWNT_{GMA}$ contents on dielectric constant of nanocomposites.

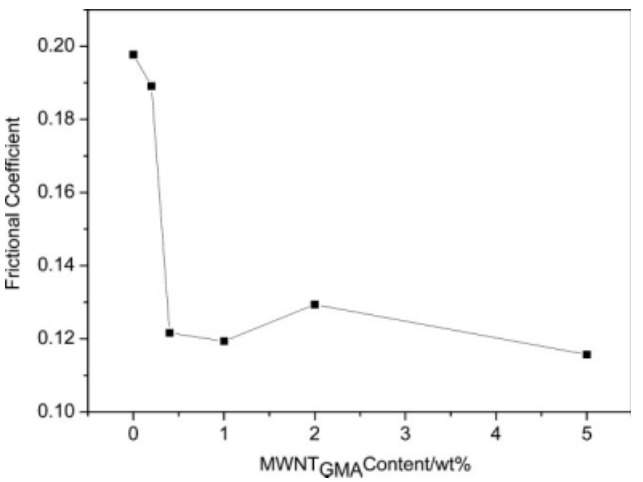

Figure 9 The effect of $MWNT_{GMA}$ contents on frictional coefficient of nanocomposites.

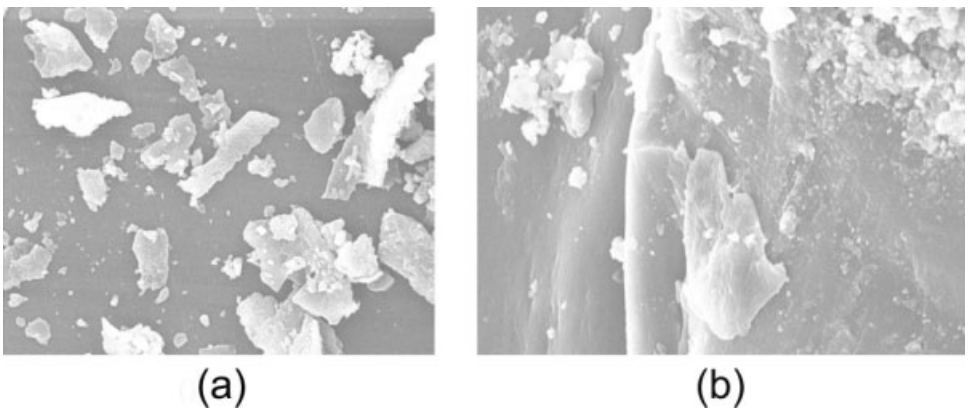

Figure 10 The SEM images of the surface of PMMA composites and MWNTs/PMMA nanocomposites: (a) $MWNT_{GMA}$ content is 0%; (b) $MWNT_{GMA}$ content is 5%.

dielectric constant. When $MWNT_{GMA}$ aggregates in polymer, the dielectric constant is decreased. It is clear from Figure 8 that with the $MWNT_{GMA}$ content increase, the dielectric loss of the $MWNT_{GMA}$/PMMA nanocomposites is somewhat increased and then decreased. When the $MWNT_{GMA}$ content is 2%, the dielectric loss factor rises from 4.7×10^{-3} of the pure system to 1.38×10^{-2}. Because there is microcapacitance structure in the nanocomposites, it will lead to the obvious increase in the dielectric loss of the nanocomposites. When the $MWNT_{GMA}$ content further increases, it is difficult to disperse in matrix, so the dielectric loss decreases.

Figure 9 shows the effects of the $MWNT_{GMA}$ with different content on the antifriction property. From the figure, it is evident that with the $MWNT_{GMA}$ content increase up to 0.5%, the friction coefficient of the nanocomposites decreases gradually from 0.20 to 0.12. When the $MWNT_{GMA}$ content increases, the friction coefficient doesn't change any more. The compatibility between GMA and PMMA improves the interfacial adhesion between polymer matrix and MWNTs, leading to a decrease in the friction coefficient of the composites.

Figure 10 shows the surface appearance of the abrasion of the PMMA nanocomposites. Because the glass transform temperature (T_g) of pure PMMA is low, there is a lot of friction chipping on the surface. The friction chipping of $MWNT_{GMA}$/PMMA nanocomposites decrease the friction chipping compared with neat PMMA (see Fig. 10). It indicates that MWNTs can reduce the friction heating temperature speed and improve the friction property. First, because of excellent strength, the $MWNT_{GMA}$ play an intensifying role in the network structure of PMMA to enhance the antifriction property of the nanocomposites. Second, $MWNT_{GMA}$ is easily to disperse in polymer matrix attributed to the C=C on the surface that participate in the polymerization of MMA and the good dispersion enhances interface strength. Load can be easily transfered between polymer and $MWNT_{GMA}$, thereby friction property is enhanced. Therefore, it can be concluded that MWNTs can significantly improve the tribological performance of the PMMA composites. The favorable effects of MWNTs on the tribological properties are attributed to unique mechanical properties and unique topological structure of the hollow MWNTs.[32]

CONCLUSION

Through the covalent bond, GMA was grafted on the surface of MWNTs. FTIR of $MWNT_{GMA}$ exhibits the carboxyl and double bond. The peak of the D pattern of $MWNT_{GMA}$ with the GMA treatment has no softening in the range of 10–20 nm. X-ray curves show that the acidification and GMA treatment does not impose influence on the graphite structure of $MWNT_{GMA}$. GMA is effectively grafted onto the MWNTs surface. The dielectric constant and the dielectric loss of the $MWNT_{GMA}$/PMMA nanocomposites gradually increase with the $MWNT_{GMA}$ content increase. With the $MWNT_{GMA}$ content increase, the friction coefficient of the nanocomposites decreases. The C=C on the surface of $MWNT_{GMA}$ participate in the polymerization of MMA enhance friction property.

The authors thank the support of Lee Feng from Shenyang National Laboratory for Materials Science, Institute of Metal Chinese Academy of Science.

References

1. Thostenson, E. T.; Chou, T. W. J Phys D: Appl Phys 2003, 36, 573.
2. Yu, M. F.; Lourie, O.; Dyer, M. J.; Moloni, K.; Kelly, T. F.; Ruoff, R. S. Science 2000, 287, 637.
3. Li, C.; Chou, T. W. Compos Sci Technol 2003, 63, 1517.
4. Peigney, A.; Laurent, C. H.; Flahaut, E.; Bacsa, R. R.; Rousset, A. Carbon 2001, 39, 507.

5. Coleman, J. N.; Blau, W. J.; Dalton, A. B.; Muñoz, E.; Collins, S.; Kim, B. G.; Razal, J.; Selvidge, M.; Vieiro, G.; Baughman, R. H. Appl Phys Lett 2003, 82, 1682.
6. Gojny, F. H.; Wichmann, M. H. G.; Fiedler, B.; Bauhofer, W.; Schulte, K. Compos: Part A 2005, 36, 1525.
7. Jin, H. J.; Choi, H. J.; Yoon, S. H.; Myung, S. J.; Shim, S. E. Chem Mater 2005, 17, 4034.
8. Ramanathan, T.; Liu, H.; Brinson, L. C. J Polym Sci Part B: Polym Phys 2005, 43, 2269.
9. Liu, Y. Q.; Yao, Z. L.; Adronov, A. Macromolecules 2005, 38, 1172.
10. Lee, K. M.; Li, L. C.; Dai, L. J Am Chem Soc 2005, 127, 4122.
11. Jiang, G. H.; Wang, L.; Chen, C.; Dong, X. C.; Chen, T.; Yu, H. J. Mater Lett 2005, 59, 2085.
12. Dyke, C. A.; Tour, J. M. J Am Chem Soc 2003, 125, 1156.
13. Chen, J.; Hamon, M. A.; Hu, H.; Chen, Y.; Rao, A. M.; Eklund, P. C.; Haddon, R. C. Science 1998, 282, 95.
14. Zhang, M. N.; Su, L.; Mao, L. Q. Carbon 2006, 44, 276.
15. Licea-Jimenel, L.; Henrio, P. Y.; Lund, A.; Laurie, T. M.; Perez-Garcia, S. A.; Nyborg, L.; Hassander, H.; Bertilsson, H.; Rychwalski, R. W. Compos Sci Technol 2007, 67, 844.
16. Georgakilas, V.; Kordatos, K.; Prato, M.; Guldi, D. M.; Holzinger, M.; Hirsch, A. J Am Chem Soc 2002, 124, 760.
17. Matyjaszewski, K.; Miller, P. J.; Shukla, N.; Immaraporn, B.; Gelman, A.; Luokala, B. B.; Siclovan, T. B.; Kickelbick, G.; Vallant, T.; Hoffmann, H.; Pakula, T. Macromolecules 1999, 32, 8716.
18. Ejaz, M.; Yamamoto, S.; Ohno, K.; Tsujii, Y.; Fukuda, T. Macromolecules 1998, 31, 5934.
19. Sano, M.; Kamino, A.; Okamura, J.; Shinkai, S. Langmuir 2001, 17, 5125.
20. Niyogi, S.; Hamon, M. A.; Hu, H.; Zhao, B.; Bhowmik, P.; Sen, R.; Itkis, M. E.; Haddon, R. C. Acc Chem Res 2002, 35, 1105.
21. Pompeo, F.; Resasco, D. E. Nano Lett 2002, 2, 369.
22. Ge, J. J.; Zhang, D.; Li, Q.; Hou, H. Q.; Graham, M. J.; Dai, L.; Harris, F. W.; Cheng, S. Z. D. J Am Chem Soc 2005, 127, 9984.
23. Zhao, B.; Hu, H.; Haddon, R. C. Adv Funct Mater 2004, 14, 71.
24. Hong, C. Y.; You, Y. Z.; Wu, D. C.; Liu, Y.; Pan, C. Y. Macromolecules 2005, 38, 2606.
25. Huang, X. Y.; Brittain, W. J. Macromolecules 2001, 34, 3255.
26. Dong, B.; Yang, Z.; Huang, Y.; Li, H. L.; Liu, L.; Yan, F. Y. J Mater Sci 2005, 40, 4379.
27. Yang, Z.; Dong, B.; Huang, Y.; Liu, L.; Yan, F. Y.; Li, H. L. Mater Lett 2005, 59, 2128.
28. Du, F.; Fischer, J. E.; Winey, K. I. J Polym Sci Part B: Polym Phys 2003, 41, 3333.
29. Zhu, L. C.; Zhang, Z.; Gao, Y. F. China Plastic Ind 2004, 32, 20.
30. Wang, Z. Y.; Jia, Z. J.; Zhang, Z. M.; XU, C. L.; Liang, J.; Zhu, S. W. Carbon Tech 1999, 103, 14.
31. Hong, C. Y.; You, Y. Z.; Pan, C. Y. Polymer 2006, 47, 4300.
32. Calvert, P. Nature 1999, 399, 210.